

A review of silo temperature field studies

ABSTRACT

Silo is a large thin-walled structure, due to the operation period will be affected by different temperatures, such as sunshine temperature difference, seasonal temperature difference and the temperature difference between inside and outside the silo wall, of which the most influential is the sunshine temperature difference, silo due to the unevenness of the temperature distribution is prone to stress concentration and more likely to occur damage. This paper briefly introduces the three-dimensional heat transfer theory and ASHRAE solar radiation model, and discusses in detail the research progress of different experts and scholars at China and abroad on the temperature effect of silos. Finally, it is concluded that there are fewer temperature regulations in China codes, and there is a need to develop a perfect temperature theory to prevent silos from damage caused by temperature inhomogeneity.

Keywords: silo; sunlight temperature difference; temperature inhomogeneity

1 INTRODUCTION

A silo is a container for storing materials supported by columns or cylinder walls and enclosed by upright silo walls[1], the form of the plane is divided into circular, rectangular, polygonal and so on. Silos are generally used for storing granular or powdered materials, and are therefore used in many fields, such as power plants, grain depots, minerals and other industries. It can be used as a structure for the regulation of production enterprises[2], as well as a warehouse for the storage of raw materials and finished products, and has the advantages of mechanization and automation. Because it belongs to the closed structure in the environmental protection play a huge role, effectively inhibit the surrounding dust pollution. The silo shape is shown in figure 1 and figure 2.



Fig. 1. reinforced concrete silo

Fig.2. steel silo

Most of the damage to silos during the operational phase occurs due to inadequate design of the wall bearing capacity. In closed circular structures, the wall forces are complex and

influenced by many factors. Among them, temperature is one of the influencing factors, including insolation temperature difference, seasonal temperature difference and temperature difference between inside and outside the silo wall. The most influential factor is the insolation temperature difference. Concrete heat transfer efficiency is low, under the effect of diurnal and seasonal temperature changes, the sunny side and the back-sunny side will cause significant differences in the temperature inside and outside the silo wall. This paper introduces the ASHRAE model, which is more commonly used to calculate solar radiation, and discusses the current domestic and international research on silo temperature field.

2 THEORY OF HEAT CONDUCTION

The transfer of heat between parts of an object without relative displacement or direct contact between different objects by the thermal movement of microscopic particles such as molecules, atoms and free electrons of a substance is called heat conduction (referred to as thermal conductivity). Thermal conductivity is due to the transfer of energy between particles or groups of particles at the atomic level and the heat transfer that occurs between the continuous medium. The essence of thermal conductivity is the amount of heat that passes from a unit area per unit time. Since the analysis of the solar radiation temperature field of the silo requires the consideration of a three-dimensional model, based on Fourier's theorem of thermal conductivity, the differential equation for the three-dimensional unsteady temperature field in Cartesian coordinate system is[3]:

$$\frac{\partial}{\partial x} \left(\lambda \frac{\partial t}{\partial x} \right) + \frac{\partial}{\partial y} \left(\lambda \frac{\partial t}{\partial y} \right) + \frac{\partial}{\partial z} \left(\lambda \frac{\partial t}{\partial z} \right) + \Phi = \rho c \frac{\partial t}{\partial \tau} \quad (1)$$

In the formula, λ is the thermal conductivity in $W/(K \cdot m)$; ρ is the density of the object in kg/m^3 ; c is the specific heat capacity of the object in $J/(kg \cdot K)$; τ is the time in s ; t is the temperature at the point (x, y, z) in $^{\circ}C$; Φ is the heat generated by the internal heat source in the unit volume per unit of time, which is called the density of the internal heat source in W/m^3 .

There are four cases below where the thermal conductivity can be simplified:

1. The thermal conductivity is constant:

The formula(1) can be reduced to:

$$a \left(\frac{\partial^2 t}{\partial x^2} + \frac{\partial^2 t}{\partial y^2} + \frac{\partial^2 t}{\partial z^2} \right) + \frac{\Phi}{\rho c} = \frac{\partial t}{\partial \tau} \quad (2)$$

$$a = \frac{\lambda}{\rho c}$$

In the formula, $\frac{\lambda}{\rho c}$ is called the thermal diffusivity or thermal diffusion coefficient.

2. The thermal conductivity is constant and there is no internal heat source:

The formula(1) can be reduced to:

$$a \left(\frac{\partial^2 t}{\partial x^2} + \frac{\partial^2 t}{\partial y^2} + \frac{\partial^2 t}{\partial z^2} \right) = \frac{\partial t}{\partial \tau} \quad (3)$$

This is a three-dimensional unsteady thermal conductivity differential equation without an internal heat source and isotropic.

3. Isotropic, steady state:

The formula(1) can be reduced to:

$$\frac{\partial^2 t}{\partial x^2} + \frac{\partial^2 t}{\partial y^2} + \frac{\partial^2 t}{\partial z^2} + \frac{\Phi}{\lambda} = 0 \quad (4)$$

Mathematically, this equation is called Poisson's equation, which is a differential equation for the temperature field of an isotropic, steady state, three-dimensional problem with an internal heat source.

4. Isotropic, no internal heat source, steady state:

$$\frac{\partial^2 t}{\partial x^2} + \frac{\partial^2 t}{\partial y^2} + \frac{\partial^2 t}{\partial z^2} = 0 \quad (5)$$

For thermal conductivity problems in cylindrical and spherical coordinate systems, the thermal conductivity equations in the corresponding coordinate systems can also be used. The equations for the cylindrical coordinate system are given below:

$$\frac{1}{r} \frac{\partial}{\partial r} \left(\lambda r \frac{\partial t}{\partial r} \right) + \frac{1}{r^2} \frac{\partial}{\partial \varphi} \left(\lambda \frac{\partial t}{\partial \varphi} \right) + \frac{\partial}{\partial z} \left(\lambda \frac{\partial t}{\partial z} \right) + \Phi = \rho c \frac{\partial t}{\partial \tau} \quad (6)$$

The equations of the spherical coordinate system are:

$$\frac{1}{r^2} \frac{\partial}{\partial r} \left(\lambda r^2 \frac{\partial t}{\partial r} \right) + \frac{1}{r^2 \sin^2 \theta} \frac{\partial}{\partial \varphi} \left(\lambda \frac{\partial t}{\partial \varphi} \right) + \frac{1}{r^2 \sin^2 \theta} \frac{\partial}{\partial \theta} \left(\lambda \sin \theta \frac{\partial t}{\partial \theta} \right) + \Phi = \rho c \frac{\partial t}{\partial \tau} \quad (7)$$

3 ASHRAE CLEAR SKY MODEL

The direction of sunlight is determined by three main physical quantities[4]: the position of the Earth's surface, the time of day, and the date. These three physical quantities can be described by the geographic latitude l , the solar time angle h , and the solar declination δ , respectively.

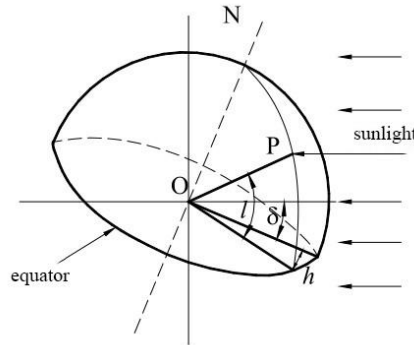


Fig.3. Latitude, solar time angle, solar declination

Let point P be the location of the project in question and the center of the earth be O. The latitude l of point P is the angle between the line OP and the projection of OP in the equatorial plane, as shown in Figure 3. Solar time angle h : the angle between the line of projection of OP

on the equatorial plane and the line connecting the center of the earth and the center of the sun projected on the equatorial plane, determined by formula(8).

$$h = (ST - 12) \times 15 \quad (8)$$

In the formula, ST is true solar time in 24 hours.

The solar declination δ is the angle between the line between the center of the Sun and the center of the Earth and its projection on the equatorial plane. Spencer[5] proposes to calculate the solar declination angle (in angles) using the following formula(9).

$$\begin{aligned} \delta = & 0.3963723 - 22.9132745 \cos N + 4.0254304 \sin N - 0.3872050 \cos 2N \\ & + 0.05196728 \sin 2N - 0.1545267 \cos 3N + 0.08479777 \sin 3N \end{aligned} \quad (9)$$

In the formula, $N = (n-1) \times 360/365$ in angular units, n is a day of the year, and $1 \leq n \leq 365$.

The sun's relative position to the earth's surface is then characterized by the sun's altitude angle β and the sun's azimuth angle ϕ , as shown in Figure 4. Solar altitude angle β : is the angle between the sun's rays and its projection on the horizontal plane, which is calculated by formula (10).

$$\sin \beta = \cos l \cosh \cos \delta + \sin l \sin \delta \quad (10)$$

The sun's altitude angle is greatest at noon and can be expressed at $\beta_{noon} = 90^\circ - |l - \delta|$.

Solar Zenith Angle θ_z : The angle between the horizon and the sun's rays. $\beta + \theta_z = 90^\circ$

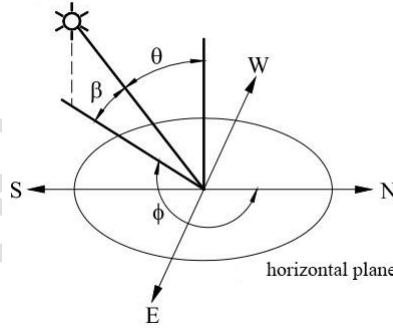


Fig.4. sun elevation angle, azimuth angle

Solar azimuth ϕ : in the horizontal plane, the projection of the sun's rays in the horizontal plane in a clockwise direction with the angle between the north direction, can also be considered that it faces the direction of the sun, calculated by the formula (11). Note that the party solves for ϕ by inverse cosine, and it is important to note in which quadrant ϕ is located.

$$\cos \phi = \frac{\sin \delta \cos l - \cos \delta \sin l \cosh}{\cos \beta} \quad (11)$$

Surface solar azimuth γ : the angle between the projection of the sun's rays on a horizontal surface and the normal to that surface for a vertical or inclined surface, as shown in Figure 5. The surface azimuth angle ψ is measured clockwise from north,

$$\gamma = |\phi - \psi| \quad (12)$$

Angle of incidence θ : the angle between the sun's rays and the direction normal to the incident surface, calculated from formula (13).

$$\cos \theta = \cos \beta \cos \gamma \sin \alpha + \sin \beta \cos \alpha \quad (13)$$

If the plane of incidence is vertical then, $\cos \theta = \cos \beta \cos \gamma$.

If the plane of incidence is horizontal then, $\cos \theta = \sin \beta$.

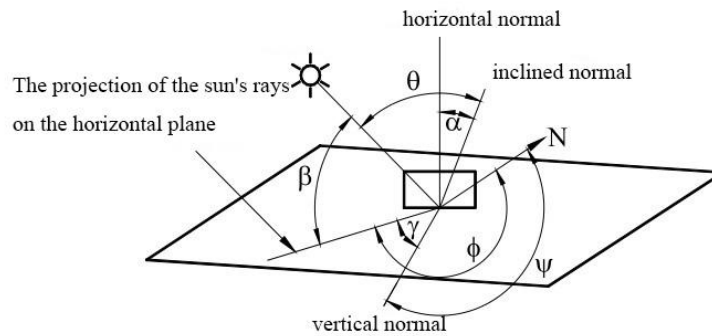


Fig.5. Surface solar azimuth, surface azimuth angle

The mean solar constant GSC is the intensity of solar radiation measured at the upper boundary of the Earth's atmosphere (the surface perpendicular to the sun's rays) at the mean Sun-Earth distance and is about 1367 W/m^2 .

Solar radiation is the thermal radiant energy on the surface of an object including absorption, reflection and transmission through a transparent object. For absorptivity α , reflectivity β , and transmittance τ there is the following relationship:

$$\alpha + \beta + \tau = 1 \quad (14)$$

The total radiation intensity G_t received by the surface of the object consists of direct radiation G_D , reflected radiation G_R , and scattered radiation G_s , which is calculated by formula (15). ϵ_0 is the absorption rate of solar radiation on the surface of the object.

$$G_t = \epsilon_0 (G_D + G_s + G_R) \quad (15)$$

Direct radiation G_D , calculated from formula (16)(17):

$$G_D = G_{ND} \cos \theta \quad (16)$$

$$G_{ND} = \frac{A}{\exp(B / \sin \beta)} C_N \quad (17)$$

In the formula, θ is the angle of incidence i.e. the angle between the sun rays and the direction normal to the incident surface.

G_{ND} is the intensity of direct solar radiation received at ground level, $\text{Btu}/(\text{h}\cdot\text{ft}^2)$ or W/m^2 ; A is the intensity of solar radiation when the mass of the atmosphere is 0, $\text{Btu}/(\text{h}\cdot\text{ft}^2)$ or W/m^2 ; B is the extinction coefficient of the atmosphere; β is the solar altitude angle; C_N is the atmospheric cleanliness.

The scattered radiation, G_d , is calculated from formula (18)(19):

For non-vertical surfaces, the

$$G_d = CG_{ND} \frac{1 + \cos \alpha}{2} \quad (18)$$

For vertical surfaces, the

$$G_d = CG_{ND} \frac{G_{dV}}{G_{dH}} \quad (19)$$

In the formula, α is the angle between the surface and the horizontal plane, C is the ratio of the

scattered radiation to the vertical incident radiation; $\frac{G_{dV}}{G_{dH}}$ is the ratio of the incident scattering from the vertical surface to the incident scattering from the horizontal surface on a sunny day, which is calculated by formula(20).

$$\frac{G_{dV}}{G_{dH}} = 0.55 + 0.437 \cos \theta + 0.313 \cos^2 \theta \quad (20)$$

The reflected radiation G_R , is calculated from formula (21):

$$G_R = G_{th} \rho_g \frac{1 - \cos \alpha}{2} \quad (21)$$

In the formula, G_{th} total radiation (direct plus scattered) falling on the horizontal or ground surface before the wall, W/m^2 ; ρ_g , reflectivity of the ground or horizontal surface.

4 STATUS OF RESEARCH

Because the silo is exposed to complex temperature effects outdoors, and because it is a thin-walled structure, the silo is more likely to encounter damage caused by temperature effects than the general building structure, and the stress analysis of the temperature effects on the silo wall in different codes is not perfect enough, if the temperature of the complex situation is encountered only with the theory of the code specified in the design is not enough, so the current research on the temperature effects of the silo is still continuing.

China's temperature research on cylindrical structures can be traced back to 1990, Li Hongyou[6] assumed that the temperatures of the back-sunny side and the points on the inner side of the cylinder are equal, and established a formula to solve the sunlight temperature stresses of cylindrical structures. YaoYangping[7] recorded the temperature data of a reinforced concrete chimney to derive the variation rule of chimney temperature with time and location, which provides reference for subsequent design and construction. Pu Weimin[8] analyzed the temperature stress of silo affected by the temperature difference between inside and outside and the temperature difference of sunshine, and put forward the calculation formula of the temperature stress of silo. Foreign research is relatively more mature, in the same year J.Y.Ooi and J.M.Rotter[9] used the Lade model to study the storage side pressure of the silo static situation and the effect of temperature on the storage side pressure. Lapko A,

Gnatowski M, Prusiel J. A [10] proposed a calculation method for calculating the temperature stress of reinforced concrete silos and verified it by theory and test. validation.

Kent [11] derived the internal force calculation formula of cylindrical shells under temperature effects along the thickness direction of the shell based on the Timoshenko shell theory, laying a theoretical foundation for studying the impact of internal and external temperature differences on silos. Briassoulis [12][13] analyzed the impact of uniform temperature effects on reinforced concrete silos. Hatfield and Bartali [14][15] studied the impact of internal and external temperature differences on reinforced concrete silos.

Priestley [16] concluded from the theory of heat conduction that the temperature difference between the inside and outside of a concrete storage tank in New Zealand under the action of solar radiation would exceed 30°C in a day, and calculated the temperature stress that would be generated by the tank under this temperature difference. Manbeck [17] analyzed the maximum temperature of the silo wall of a steel silo in North America under the action of solar radiation. The analysis concluded that the temperature of the silo increased by 10-24°C/h due to the action of solar radiation.

Due to the main purpose of silos is storage, the change of side pressure of the silo wall caused by temperature effects is an important research direction. Anderson [18] first proposed in 1966 that when the silo wall shrinks due to the decrease of ambient temperature, the internal storage of the silo cannot shrink in time, resulting in an increase in side pressure of the silo wall due to the limitation of the internal storage of the silo. Moran [19][20] et al. used ANSYS to simulate the side pressure of steel silos under uniform negative temperature, and the constitutive model of the storage material was Drucker-Prager model. The conclusion was that when the temperature drop exceeded 20°C, the side pressure of the silo wall would be greater than the side pressure value specified in the code.

Ma Lisha [21][22] Thermal coupling analysis of prestressed silo, the results show that the specification of the seasonal cooling temperature stress should be taken as 6% of the circumferential stress can not meet the safety requirements, it is recommended to take the circumferential stress of more than 8% calculation. Zhang Shaokun [23] study concluded that the important factor affecting the increase of silo stress is the temperature difference between inside and outside, the greater the temperature difference, the greater the displacement and stress of the silo, it is recommended to increase the silo wall circumferential reinforcement to ensure structural safety. Xiang Shihai [24] The stress analysis of silo under different working conditions, the results of the surface temperature change on the radial stress and vertical stress of the silo has a small effect, the effect on the circumferential stress is larger.

Meng Shaoping [25] used the theory of cylindrical shells with moments to derive the formula for calculating the internal force of the silo wall under the action of storage material and temperature, and calculated that the ratio of the maximum circumferential stresses under the action of temperature and storage material load decreases with the increase of the silo diameter. Han Chongqing [26] et al. analyzed the calculation of a 60m diameter silo and concluded that the temperature stress of large diameter silo is mainly affected by the wall thickness, and the most unfavorable position of the silo wall is not at the bottom, but at a certain height from the ground. Xia Dongtao [27][28] et al. carried out finite element analysis of a 120m diameter reinforced concrete coal storage silo under the influence of ambient temperature, and studied the wall stresses under different conditions, and concluded that the

annular stress in the temperature drop condition when the silo is empty is about 7 times of the temperature rise condition, and the annular stress of the silo wall in the temperature rise condition when the silo is full is about 30% of that in the temperature drop condition, and suggested that for the giant silos with diameters greater than 100m, the maximum annular tension should be taken as 30%-50% to calculate their temperature stresses. 30%-50% of the maximum ring pull force is recommended to calculate the temperature stress. Zhou Yongqiang et al.[29] carried out finite element analysis on a 120m diameter indoor reinforced concrete silo and concluded that under temperature loading, there are large internal forces and displacements in the structure and the lower and middle part of the silo wall is the most important place to be strengthened. Liu Min[30] Simulation of a silo under storage pressure and temperature difference between inside and outside of the silo was carried out, and it was concluded that the temperature difference effect has a great influence on the bending moment of the silo.

Wang Liu[31], Zhang Bo[32] analyzed the field experiment and simulation of the temperature of a silo with a diameter of 33.6m and a height of 41.4m in the construction period and the operation period, and concluded that the maximum internal and external temperature difference value is 7.2°C in the construction period, and the maximum temperature difference between the sunny side and the backside is about 5°C in the operation period. Liu Hongbo et al.[33] proposed a method to calculate the shadow zone of solar radiation for uncovered silos, and verified the reasonableness of their method by experimental modeling, and the influence of solar radiation on the actual project should be strictly considered in the design. Yang Yinghua, Ma Yue[34][35] adopted the ASHRAE clear sky model to analyze the stress results of steel silos under different insolation temperatures, and concluded that the circumferential and axial stresses at the bottom of the silo are the largest when subjected to solar radiation, and that the locations of the maximum stresses appear differently when different insolation temperatures are applied. Ma Yue et al.[36][37] simulated the temperature of a variable wall thickness steel silo at the summer and winter solstices. In the case of empty silo, the circumferential temperature difference will be more than 30°C, while in the case of full silo, the circumferential temperature difference will be less than 20°C, and the temperature stress generated by solar radiation is mainly concentrated at the top and bottom of the silo. Zhao et al.[38] analyzed the measured data of a silo with a height of 23.38m and a diameter of 46.4m in Hubei province, which showed that the outer surface temperature of the silo mainly receives the influence of solar radiation and ambient temperature, and came to the conclusion that the temperature effect of the analysis of the large-diameter concrete silos is not as large as the temperature effect of the solar radiation and ambient temperature. It is more practical to analyze the temperature effect of large diameter concrete silo along the wall thickness of the nonlinear distribution. The wall thickness has a significant effect on the temperature effect. Chen[39], Jiang Long[40], Li Yutao[41] et al. conducted on-site temperature and stress monitoring and numerical simulation for a silo with a diameter of 136.5m and a height of 19.35m, and investigated the effects of insolation and seasonal temperature changes on the stresses. Under the influence of the two temperature modes, the temperature profile and stress profile showed an anti-symmetric situation. In the case of insolation, the large temperature change of the outer surface leads to obvious stress change on the outer side, and

the stress of the annular reinforcement on the sunny side is 10-20 MPa larger than that on the back-sunny side in summer, which is more likely to cause concrete cracking.

5 CONCLUSION

Silo this large annular thin-walled structure, by the temperature of the great influence, domestic and foreign experts and scholars in the temperature stress of the silo have a certain degree of progress. However, our specification for the temperature stress is less, cannot effectively solve the effect of temperature on the silo, must be based on existing field data or simulation analysis, comprehensive consideration of different temperatures on the internal force of the silo wall, to develop a detailed and reasonable theory of the silo temperature, in order to prevent the silo by the damage caused by the temperature inhomogeneity, but also need to experts and scholars of the hard work.

REFERENCES

1. GB 50077-2017, Reinforced concrete silo design standard [S]. Beijing: China Planning Press, 2017.
2. Dong Chuanbo. Research on the introduction and safe operation technology of large coal storage silo in harbor[C]. Proceedings of the 2017 Annual Conference of National Metallurgical Automation Information Network, 2017: 216-219.
3. Tao Wequan. Heat transfer [M]. Beijing: Higher Education Press, 2019
4. McQuiston FC, Parker JD, Spittler J.D. Heating, Ventilation and Air Conditioning [M]. Yu Bingfeng, Translation. Beijing: Chemical Industry Press, 2005.
5. J. W. Spencer, Fourier Series Representation of the Position of the Sun, Search, Vol. 2, No. 5, p. 172, 1971
6. Li, Hongthalein. Study on the effect of sunlight on high-rise building structures[J]. Engineering Mechanics, 1990, 7(3): 65~82.
7. Chen Bingxin, Yao Yangping. Statistical distribution of insolation temperature in reinforced concrete chimneys[J]. Journal of Civil Engineering, 1992, 6: 58~65.
8. Kong Derui, PuWiemin. Temperature effects on a 40 m diameter cylindrical silo. Special Structures, 1998(12): 32-38.
9. J. Y. Ooi and J. M. Rotter. wall pressure in squat steel silos from simple finiteelement analysis[J]. Computers & structures, 1990.
10. Lapko A, Gnatowski M, Prusiel J. A. Analysis of some effects caused by interaction between bulk solid and r. c. silo wall structure[J]. Powder Technology, 2003, 133(1~3): 44~53.
11. Kent C H. Thermal stresses in thin-walled cylinders[M]. University of Michigan, 1931.
12. Briassoulis D, Curtis J O. Effect of End Restraints and Forces on the State of Stress in Circular[J]. Transactions of the ASAE, 1985, 28(1): 222-0231.
13. Briassoulis D, Curtis J. Design and analysis of silos for friction forces[J]. Journal of Structural Engineering, 1985, 111(6): 1377-1398.
14. Hatfield F J, Bartali E H. Static forces and moments in a grain silo[J]. Journal of Structural Engineering, 1988, 114(12): 2814-2819.

- 15 Bartali E H, Hatfield F J. Forces in cylindrical grain silos caused by decreasing ambient temperature[J]. ACI Structural Journal, 1990, 87(1):108-116.
- 16 Priestley M J N. Ambient thermal stresses in circular prestressed concrete tanks[J]. ACI Journal. 1976, 73(10): 553-560.
- 17 Manbeck H B, Britten M G. Prediction of Bin-Wall Temperature Declines[J]. Transactions of the ASAE, 1988, 31(6): 1767-1773.
- 18 Andersen P. Temperature stresses in steel grain storage tanks[J]. Civil Engineering ASCE, 1966, 36(1): 74.
- 19 Moran J M, Juan A, Ayuga F, et al. Analysis of thermal load calculations in steel silos: A comparison of Eurocode 1, classical methods, and finite element methods[J]. Transactions of the ASAE, 2005, 48(4): 1483-1490.
- 20 Moran J M, Juan A, Robles R, et al. Effects of environmental temperature changes on steel silos[J]. Biosystems engineering, 2006, 94(2): 229-238.
21. Ma Lisha. Research on circular silo under the action of ambient temperature [D]. [Master's thesis]. Xi'an: Xi'an University of Architecture and Technology, 2015.
22. Ma Lisha. Research on circular silo under the action of ambient temperature[J]. Specialty Structures, 2016, 33(5): 6-9.
23. Zhang Shaokun. Finite element analysis of temperature load and storage load effects on large diameter reinforced concrete silo [D]. [Master's thesis]. Wuhan: Wuhan University of Technology, 2008.
24. Xiang Shihai. Research on temperature effect of large diameter cylindrical silo [D]. [Master's thesis]. Zhengzhou: North China University of Water Conservancy and Hydropower, 2014.
25. Sun Weiwei, Meng Shaoping, Luan Wenbin. Parametric analysis of temperature stress in the wall of large diameter concrete silo[J]. Special Species Structure, 2009, 3: 58-60.
26. HAN Chongqing, MENG Shaoping. Study on the temperature effect of 60m diameter cement clinker silo[J]. Industrial Building, 2000, pp.30.4: 58-60.
27. Xia Dongtao, Xu Lihua. Analysis of the effect of ambient temperature action on the internal force of giant coal storage silo[J]. Industrial construction Building, 2006, 36.3: 80-82.
28. XIA Guangzheng, XIA Dongtao. Finite element analysis of giant coal storage silo under ambient temperature[J]. Space junction
The Organization for Economic Cooperation and Development, 2006, 12.1: 62-64.
29. ZHOU Yongqiang, GAO Zhengguo. Finite element analysis of giant coal storage silo[J]. Industrial Building, 2008, z1: 351-355.
30. Liu Min. Research on structural design technology of prestressed concrete coal storage silo [D]. 2012. Master's thesis. Southwest Jiaotong University.
31. Liu Wang. Evolution analysis of force performance during construction of large diameter prestressed silo [D]. North China University of Water Resources and Hydropower, 2021.
32. Zhang Bo. Study on time-varying stress performance of prestressed concrete coal storage silo during operation period [D]. North China University of Water Resources and Hydropower, 2022.
33. Liu Hongbo, Zhang Zhisheng, Chen Zhihua et al. Research on temperature field and temperature effect of steel plate silo under solar radiation[J]. Journal of Building Structures, 2016, 37(08): 151-157.

34. YANG Yinghua, MA Yue. Stress analysis of large-diameter alumina steel silo under insolation temperature[J]. Building Structure, 2014, 44(12): 104-109.
35. Ma Yue. Analysis of the effect of insolation on the structural performance of large-diameter floor-standing steel silos [D]. Xi'an University of Architecture and Technology, 2013.
36. Ma Yue, Yang Hongxia. Structural thermal response of steel silo with variable wall thickness under solar radiation[J]. Journal of Yan'an University (Natural Science Edition), 2020, 39(04): 58-62.
37. MA Yue, YANG Yinghua. Temperature field distribution of large-diameter floor-standing silo structures under solar radiation[J]. Space Structure, 2016, 22(04): 71-77.
38. Zhao Liang, Yang Zhiyong, Wang Lijie. Investigation on the Non-Uniform Temperature Distribution of Large-Diameter Concrete Silos under Solar Radiation[J]. Mathematical Problems in Engineering, 2018, 2018.
39. Chen Z, Li X, Yang Y, et al. Experimental and numerical investigation of the effect of temperature patterns on behavior of large scale silo[J]. Engineering Failure Analysis, 2018, 91: 543-553.
40. Jiang Long. Research on temperature effect of large diameter silo in severe cold area [D]. North China University of Water Conservancy and Hydropower, 2014.
41. Li Yutao. Temperature stress monitoring analysis of large diameter reinforced concrete silo in cold region [D]. North China University of Water Resources and Hydropower, 2014.